Computers and Concrete, *Vol. 22, No. 6 (2018) 515-525*
DOI: https://doi.org/10.12989/cac.2018.22.6.515

Performance of bridge structures under heavy goods vehicle impact

Wuchao Zhao[1a], Jiang Qian[*1] and Juan Wang[2b]

[1]*State Key Laboratory of Disaster Reduction in Civil Engineering, Tongji University, Shanghai 200092, China*
[2]*Business School, Shanghai Jian Qiao University, Shanghai 201306, China*

(Received March 12, 2018, Revised December 7, 2018, Accepted December 11, 2018)

Abstract. This paper presents a numerical study on the performance of reinforced concrete (RC) bridge structures subjected to heavy goods vehicle (HGV) collision. The objectives of this study are to investigate the dynamic response and failure modes of different types of bridges under impact loading as well as to give an insight into the simplified methods for modeling bridge structures. For this purpose, detailed finite-element models of HGV and bridges are established and verified against the full-scale collision experiment and a recent traffic accident. An intensive parametric study with the consideration of vehicle weight, vehicle velocity, structural type, simplified methods for modeling bridges is conducted; then the failure mode, impact force, deformation and internal force distribution of the validated bridge models are discussed. It is observed that the structural type has a significant effect on the force-transferring mechanism, failure mode and dynamic response of bridge structures, thus it should be considered in the anti-impact design of bridge structures. The impact force of HGV is mainly determined by the impact weight, impact velocity and contact interface, rather than the simplification of the superstructure. Furthermore, to reduce the modeling and computing cost, it is suggested to utilize the simplified bridge model considering the inertial effect of the superstructure to evaluate the structural impact behavior within a reasonable precision range.

Keywords: RC bridges; HGV; impact analysis; redundancy; simplified methods; dynamic response

1. Introduction

As the number of vehicle-bridge collision accidents, terrorist attacks and other impact events rapidly increase during the past two decades, the safety of bridge structures under extreme loadings has been highlighted by many scholars. Wardhana and Hadipriono (2003) conducted an investigation of 503 bridge collapse accidents occurred in the United States between 1989 and 2000, and concluded that vehicular collisions were the third-leading factor causing bridge failure. The same conclusion was drawn by Cook *et al*. (2013) in the statistics of the 92 bridge collapse for New York City from 1987 to 2011, of which about 19.2% were due to the lateral impact loading. Ji and Fu (2010) reported that about 15.30% of bridge collapse accidents in the service stage were caused by impact actions of vehicles and vessels in China. It can be found that the vehicular collision is a serious threat to the safety of bridge structures. Due to the severe consequences of the structural failure, the study on the impact mechanism of bridges is of great significance.

In this situation, a great deal of effort has been made to investigate the impact action on the bridge structures. Sharma *et al*. (2012) carried out the numerical simulations on the collision between the bridges and vehicles with different velocities to examine the shear demand of the RC columns. The simulation results demonstrated that the resistance mechanism of the bridge under vehicle impact is based on the shear, inertia, and local deformation. Thus, the dynamic peak impact force is an important factor for the damage level of RC columns. An extensive parametric study of 13 parameters was carried out by Abdelkarim and ElGawady (2017) to explore the peak impact force and the equivalent force of the vehicle collision with bridge pier. In order to obtain the collision force effectively and reduce the computational cost, a coupled mass-spring-damper model was proposed by Chen *et al*. (2016) based on numerous detailed finite element analysis.

However, Lu *et al*. (2013) analyzed the impact force of different truck types collided with the bridge superstructure, and the results indicated that the impact forces between the vehicles and the bridges mainly depend upon the vehicle parameters. Buth and his co-workers (2010, 2011) documented 19 typical cases of bridge failures caused by the collision action of truck-tractor-trailers. Besides, the numerical and experimental studies to evaluate the impact force of HGV on bridge piers were carried out. The tested results were adopted by the AASHTO-LRFD bridge design provisions (2012). A lot of bridge collision accidents also showed that the impact action of HGV is one of the main reasons behind the failure of bridges. To date, the FE models of light and medium-duty vehicles have been widely used to investigate the dynamic response of vehicle-bridge collision (El-Tawil *et al*. 2005, Chung *et al*. 2013, Yi *et al*. 2015, Chen *et al*. 2016, Abdelkarim and ElGawady 2017, Kang and Kim 2017). However, to the author's knowledge,

∗Corresponding author, Professor
E-mail: jqian@tongji.edu.cn
[a]Ph.D. Student
E-mail: zwuchao219@126.com
[b]Assistant Professor
E-mail: daphnei@163.com

ISSN: 1598-8198 (Print), 1598-818X (Online)

HGV FE models are rarely used in vehicle-bridge collision.

Some current design specifications (JTG D60-2004 2004, British Standards Institution 2006, AASHTO-LRFD 2012) usually employ the equivalent static force method to evaluate the impact capacity of the bridge components; however, the redundancy of bridge structures and the dynamic effect of the impact actions were not yet taken into consideration. Single-column and multicolumn bridge structures are the most common structural types in the urban areas, and the two kinds of structures under vehicle impact may have some difference in the impact behavior. Therefore, there is an urgent need to study the performance of bridges with different substructure types for deepening the understanding of the vulnerability of bridges under vehicle collision.

In addition, the detailed finite-element analysis on the impact force between vehicle and bridge pier was firstly conducted by El-Tawil *et al*. (2005). It is indicated that the dynamic response of the bridge structure is not sensitive to the stiffness of the bearing, and other components of the bridge structure have no time to respond as the impact duration is too short. In order to reduce the cost consumed in the modeling and calculating, simplified methods for the superstructure are proposed by many scholars (Thilakarathna *et al*. 2010, Sha and Hao 2012, Sharma *et al*. 2012, Yi *et al*. 2015, Abdelkarim and ElGawady 2016). The dynamic response and failure modes of the simplified models subjected to vehicle collision are bound to be different; nevertheless, little work has been conducted to discuss the effects of simplified methods on the performance of bridge structures.

The present study aims to thoroughly analyze the performance of different bridge structures subjected to HGV collision to contribute new information on the impact mechanism of bridge structures. In addition, the effect of simplified methods for modeling the superstructures on the dynamic response of the bridge structures is also examined. To ensure the reliability and accuracy of the numerical results, the FE models are validated against an experimental result as well as an actual collision accident. The impact force, displacement, internal force distribution and failure mode of bridge models subjected to HGV collision are discussed in depth.

2. Finite element modeling

2.1 Bridge models

The main research object of this paper is the reinforced concrete single-column and double-column bridge structures, which have been widely used in urban areas. The double-column bridge had been established by the authors, and the modeling details can be referred to the previous literature (Qian *et al*. 2016). Thus, only the FE model of the single-column bridge is presented here.

2.1.1 Bridge configuration

A typical single-column bridge with pier, bent, girder and bearing is adopted herein, as presented in Fig. 1. The pier has a circular cross section with the diameter of 1200 mm, and the pier height is 6000 mm equal to that of the double-column bridge. The diameter of longitudinal reinforcements is 32 mm with a yield strength of 400 MPa, and the reinforcement ratio is 1.13%. The 16 mm steel bars with a yield strength of 335 MPa are utilized as stirrups spaced at 200 mm. The bent dimension is 4000 mm × 1500 mm × 1500 mm (length × width × height), and the superstructure is assigned a weight of 2600 kN. In order to reduce the modeling costs, the girder is simplified as a rigid mass block. The superstructure gravity load is transmitted to the pier through two elastomeric pads with a dimension of 500 mm × 500 mm × 50 mm; and the friction coefficients among the pier, girder, and rubber bearings are taken as 0.3 (JTG D60-2004 2004).

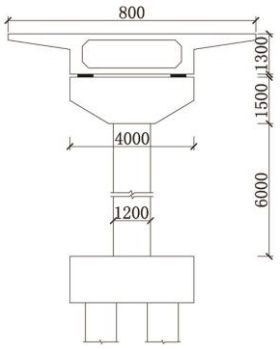

Fig. 1 Configuration of the single-column bridge (unit:mm)

2.1.2 Material model

Material model has a significant effect on the nonlinear analysis results. Many constitutive models of concrete are available in LS-DYNA. However, the continuous surface cap model named *MAT_CSCM_CONCRETE (Murray *et al*. 2007) is utilized in this study to simulate concrete behavior, including elastic update, plastic update and yield surface definition, damage, rate effects, and kinematic hardening. As shown in Fig. 2, the failure surface is plotted as the shear strength versus pressure, and a smooth and continuous intersection is formulated between the failure surface and hardening cap. Although originally developed for the analysis of roadside safety structures, this model has been successfully used for the dynamic analysis of the bridge structures under vehicle collision. This model provides a convenient option for inputting data, where the default parameters are provided by the code through three inputs: unconfined compressive strength, aggregate size and the units. In this study, the aggregate size of concrete is set as 20 mm.

The mass block on the top of the pier is assumed to be rigid and simulated with MAT_RIGID (MAT_20) model, which is very efficient as rigid elements are bypassed in the element processing, and no storage is allocated for storing history variables. The material density is adjusted to make the block weight equal to the weight of the superstructure assigned to the pier.

The bilinear elasto-plastic model named *MAT_PLASTIC_KINEMATIC is employed to simulate the reinforcement, where the strain rate effect needs to be considered. In this study, the plastic hardening modulus is assumed as 1%

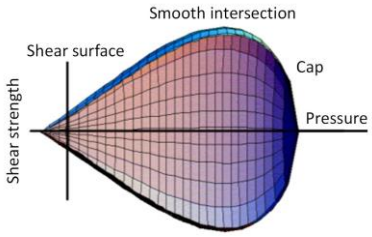

Fig. 2 Yield surface shape of CSCM

Table 1 Material parameters of the bridge model

Material	Elastic modulus (MPa)	Density (kg/m^3)	Poisson's ratio	Ultimate strength (MPa)	Yield strength (MPa)
Concrete	3.25×10^4	2380	0.2	26.8	—
Steel bars	2.00×10^5	7850	0.3	—	400
Stirrups	2.00×10^5	7850	0.3	—	335

of elastic modulus. In addition, the strain rate effect is accounted for using the Cowper-Symonds model (Jones 2011), which scales the yield stress by the strain rate dependent factor as follows

$$\frac{\sigma_y^d}{\sigma_y^s}=1+\left(\dot{\varepsilon}/D\right)^{1/q} \tag{1}$$

Where σ_y^d is the dynamic flow stress at an uniaxial plastic strain rate $\dot{\varepsilon}$, σ_y^s is the associated static flow stress. The values of 40.4 and 5 are used for *D* and *q*.

The material properties of the pier model are listed in Table 1.

2.1.3 Bridge models

Eight-node solid elements (SOLID164) with one integration point (i.e., constant stress formula-tion) are selected for simulating the pier concrete to reduce the calculating time; and the virtual hourglass control (based on the Flanagan-Belytschko approach (Flanagan and Belytsch-ko 1981)) is also applied to avoid the excessive hourglass energy. After the careful convergence check, the mesh size of concrete element is set as 0.1 m (Sha *et al*. 2012, Wang and Morgenthal 2017). The reinforcements are simulated by Hughes-Liu beam elements (BEAM161). In addition, the Lagrangian coupling method is implemented with the keyword *CONSTRAINED_LAGRANGE_IN_SOLID for modeling the perfect bond between concrete and reinforce-ments (LS-DYNA 2007). The accuracy of this method has been confirmed by comparing the analytical and numerical results (Moutoussamy *et al*. 2011). As it is not necessary to match the nodes between the concrete and reinforcements, the complexity of the modeling process can be avoided. The rubber bearings are simulated by 8-node solid elements with Blatzko-Rubber material, and the shear modulus is assigned as 1.2 MPa (JTG/T B02-01-2008 2008). The piers of bridge models are assumed to be fixed in all directions at the bottom section. The FE models of single-column and double-column bridge structures are shown in the Fig. 3.

2.2 HGV model

(a) Single-column bridge (b) Double-column bridge

Fig. 3 Finite element models of the bridge

(a) Original HGV (b) Modified HGV

Fig. 4 Finite element model of the tractor-trailer truck

A detailed finite element model of truck-tractor-trailer is used in the impact analysis, as shown in Fig. 4(a), which is provided by the National Crash Analysis Centre (NCAC) of George Washington University. The 38-ton vehicle model is a 5-axle (1+1+3) articulated heavy goods vehicle designed to simulate TB81 test, according to European Standard EN1317 (European committee for standardization 1998). In order to simulate the common container truck in China, the trailer of the FE model is modified as a 40-foot standard container as shown in Fig. 4(b). The container is simulated by beam elements and shell elements (Madurapperuma and Wijeyewic-krema 2013), while the cargo is modeled by solid elements with the elastic material. As the stiffness of the cargo has a significant effect on the impact force (Buth *et al*. 2010), the elastic modulus of the cargo is taken as 1000 MPa in this study, which is slightly less than 2000 MPa suggested by Chen *et al*. (2016). According to the Chinese road traffic laws, the maximum allowable speed of HGV is 75-100 km/h, hence the impact velocities are taken as 40 km/h, 60 km/h, 80 km/h and 100 km/h in the present study of the vehicle-bridge collision. In addition, the mass of HGV is in the range of 30 tons to 40 tons.

As the vehicle-bridge collision involves the strong contact nonlinearity, the simulation method for the slip, contact and self-contact between the elements has a great influence on the calculation results. Here the contact algorithm named *CONTACT_AUTOMATIC_SINGLE_SURFACE_ID in LS-DYNA is employed between the vehicle and bridge models; and the dynamic and static coefficients of friction between the contact surfaces are taken as 0.3 (El-Tawil *et al*. 2005).

2.3 Validation of the numerical models

The modified HGV FE model is validated by comparing the numerical results with a full-scale crash test result conducted by Buth *et al*. (2011). The HGV weight is adjusted to 36 tons by changing the cargo density, and a

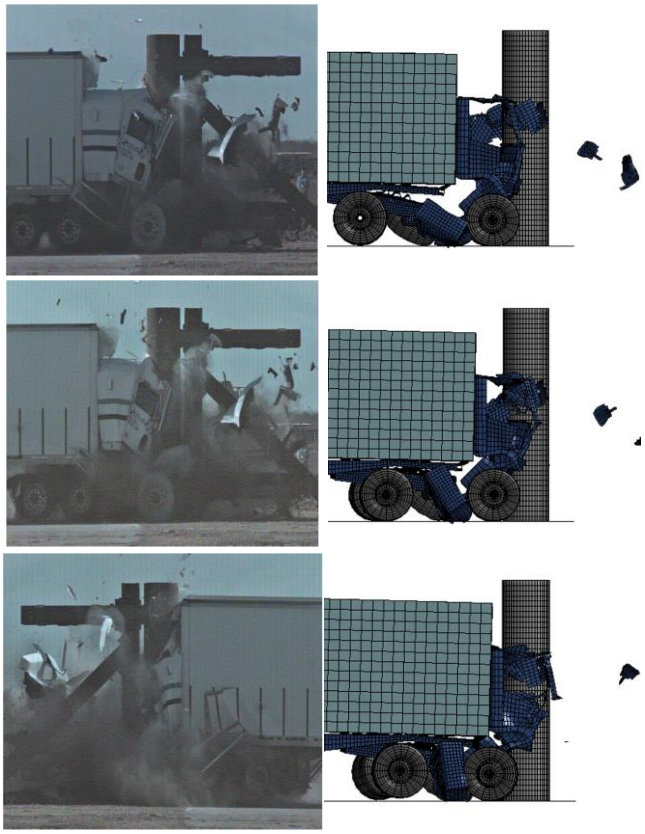

(a) Vehicle crash test (b) Numerical simulation

Fig. 5 Validation for the HGV model

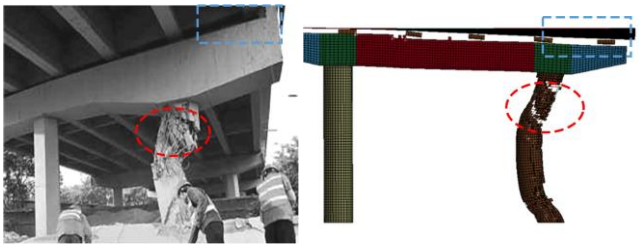

(a) Truck collision accident (b) Numerical simulation

Fig. 6 Validation for the bridge model

rigid pier with a diameter of 0.91 m is also established. Fig. 5 shows the comparison of the HGV damage states between the experimental result and simulation result at different impact time. It can be observed from this figure that the HGV FE model can well reproduce the damage state of the truck in the crash test, which demonstrates the FE model of HGV has certain reliability.

The accuracy of the bridge finite element model is verified by comparing the failure mode of the bridge with an actual collision accident. It was an overloaded truck hitting the pier of an overpass bridge in Guangzhou, China, on January 17, 2010. The truck impact action caused the serious damage of the pier, and the deck of the bridge also seriously tilted, even though the bridge structure did not collapse. As the design parameters of the bridge are unknown, the failure mode of the established double-column bridge FE model subjected to the modified HGV collision is used to compare with the accident. The comparison of the bridge failure mode between the numerical simulation and the actual traffic accident is shown in Fig. 6, where a good agreement on the failure mechanism of the bridge structures subjected to vehicle collision can be observed.

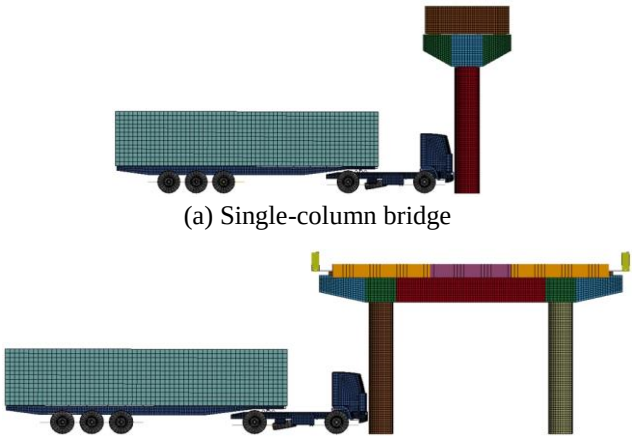

(a) Single-column bridge

(b) Double-column bridge

Fig. 7 FE models for collision simulations

Based on the verification of the HGV and bridge FE models, sufficient confidence is provided for constitutive model, contact, boundary and other parameters in the numerical models. It indicates that the FE models in the present study have the capacity to reproduce the failure mode and dynamic response of the system, which will be utilized in the following impact analysis.

3. Crashworthiness of different bridge structures

Fig. 7 presents the FE models utilized to analyze the dynamic responses of different bridge structures during the vehicle collision. In order to avoid the large initial penetration, the initial distance between the bumper of HGV and the bridge pier is set to be 50 mm. The impact velocities of the HGV are set as 40, 60, 80 and 100 km/h, respectively; and the weight of the HGV is ranging from 30 tons to 40 tons by changing the cargo density.

3.1 Failure modes

Fig. 8 shows the failure modes of the single-column and double-column bridges under the impact action of the 40-ton truck with different velocities. In low impact velocity cases, the initial impact force is resisted by the inertial force, and the piers only suffer minor local damage at the impacted region and the pier base. This is mainly because the bridge piers are stiffer than the vehicle bumper and frontal rail which absorb most of the initial kinematic energy. In this case, the damage states of the two bridge models are almost identical. However, when the truck impacts the piers at a higher velocity, a larger inertial force is triggered by the impact action, resulting in a significant plastic deformation at the base of the impacted piers. The resistance mechanism of the single-column bridge in the collision process mainly depends on the reaction force of

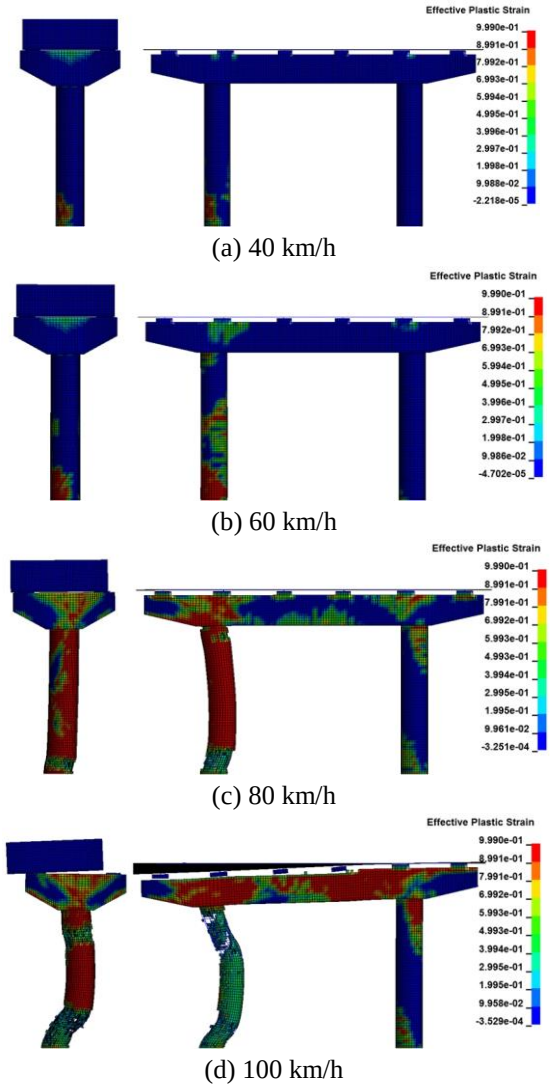

(a) 40 km/h

(b) 60 km/h

(c) 80 km/h

(d) 100 km/h

Fig. 8 Failure modes of the bridges under impact

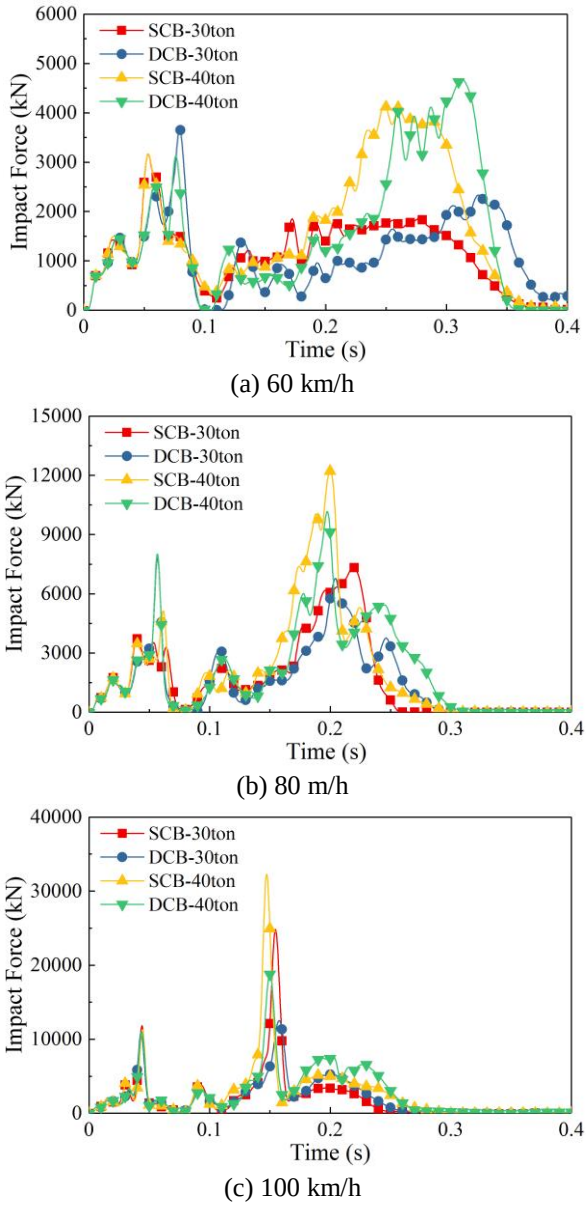

(a) 60 km/h

(b) 80 m/h

(c) 100 km/h

Fig. 9 Time histories of impact force at different velocities

the bottom fixed end and the inertial force of the structure. The impact resistance of the double-column bridge is provided by the support ends of two piers and the inertial forces of components. In the high-velocity cases, both ends of impacted piers are seriously damaged.

As the impact duration is so short that the other components have no time to response, the damage mainly concentrates on the impacted piers in the early impact stage. However, the other components play an important role on the overall response of the structures in the subsequent response stage. Due to the difference in the structural redundancy, the single-column bridge may collapse directly as a result of the serious damage of the pier at the base under HGV collision, while the double-column bridge can delay the overall collapse of the structure due to the supporting of the second pier.

The dynamic response of bridge superstructures should be taken into consideration in the vehicle-bridge collision analysis, as it directly relates to the structural stability. When the impact velocity is low, the response of the superstructure is rather small due to its inertial effect and the vibration isolation effect of the bearing. Furthermore, the superstructure has no time to response to the vehicle impact action when the impact velocity is over 80 km/h. It also should be noticed that a large axial deformation of the pier is triggered by the large lateral displacement. In this case, a relative slip or a serious detachment between the superstructure and the pier may occurs. In addition, the axial deflection of the pier may cause the bearings failure. Thus, it can be stated that the safety of bearing and the stability of the superstructure are strongly affected by both the horizontal and vertical displacements of the pier head. Furthermore, the tensile-shear failure model is observed near the top of the impacted pier.

3.2 Impact force time histories

The impact force time histories of the bridges under different impact velocities are shown in Fig. 9. The SCB and DCB, presented in this figure, are short for the single-

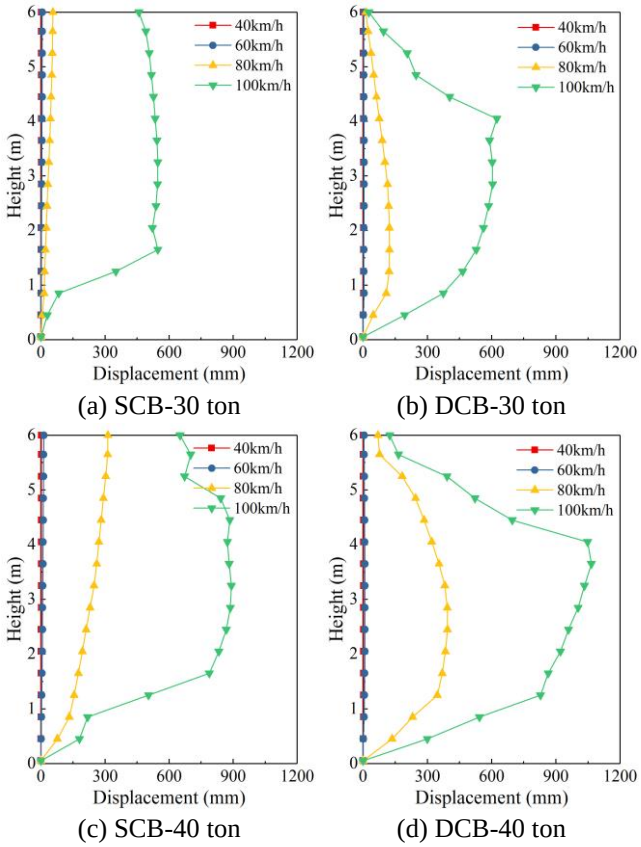

(a) SCB-30 ton (b) DCB-30 ton

(c) SCB-40 ton (d) DCB-40 ton

Fig. 10 Deformation profiles of the pier along the height

column and double-column bridge, respectively. It can be found that the peak impact forces increase with the HGV velocity and mass, and the impact force time histories vary greatly with different initial kinematic energy. Two spikes occur in the time history of impact force due to the collision between the engine, cargo of the truck and the piers. When the impact velocity exceeds 80 km/h, the second spike of the impact force is much larger than the first one. It is indicated that the cargo impact action dominates the peak impact force rather than the engine, which is quite different from that of the light vehicle. Therefore, the impact response of the system can be divided into two stages: the engine impact stage and the cargo impact stage.

3.3 Deformation profile

Fig. 10 shows the deformation profiles of the impacted piers along the height under different impact cases. When the impact velocity is lower than 60 km/h, the lateral displacements of the impacted piers are very small. In this case, the HGV impact action has little effect on the overall response of the bridge structure. However, when the impact velocity is higher than 80km/h, the piers generate larger lateral displacement, and the damage of the piers are serious. It can be found that the pier displacement of the double-column bridge is bigger than that of the single-column bridge, which is mainly determined by the section stiffness. Due to the different top boundary conditions of the piers, there is a big difference in the pier deformation profile of the two bridge models. The maximum lateral

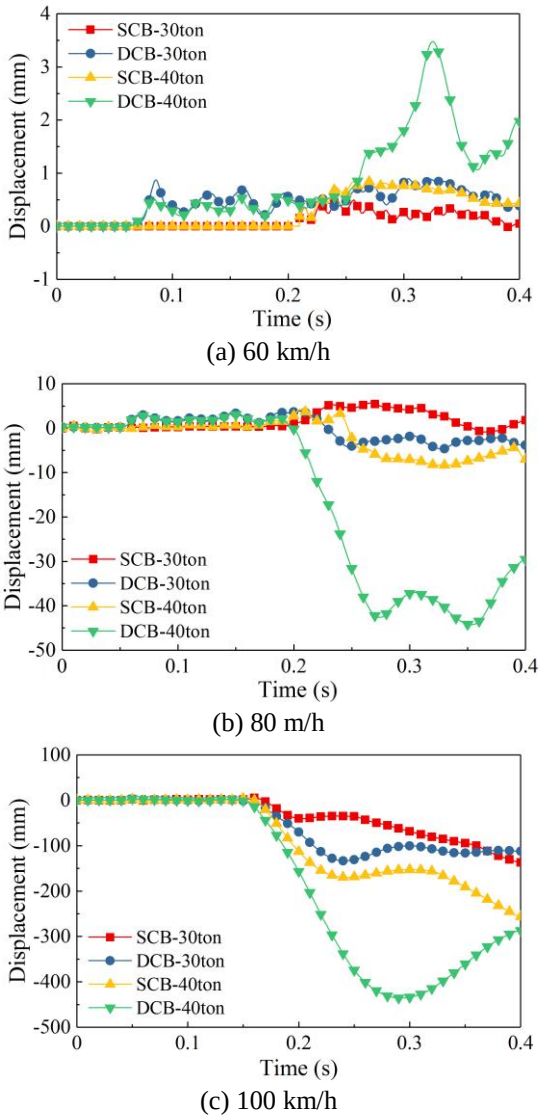

(a) 60 km/h

(b) 80 m/h

(c) 100 km/h

Fig. 11 Axial displacement time histories of impacted piers

displacement of the single-column bridge is often distributed at the impact point or the top of the pier; however, the maximum displacement of the double-column bridge piers usually occurs at the impact point. It is apparent that the top lateral displacement of the single-column bridge is much larger than that of the double-column bridge, indicating that the single-column bridge under HGV collision is more prone to generate a slip or detachment between the superstructure and the pier. Moreover, it should be noted that the position of the maximum lateral displacement is getting higher with the increase of the impact velocity, which is greatly related to the cargo impact action.

The axial displacement time histories of the pier under 40-ton truck collision at initial velocities of 60 km/h, 80 km/h and 100 km/h are presented in Fig. 11. With the propagation of stress wave and the development of shear cracks in concrete, the length of the impacted piers in the impact process tends to increase when the initial velocity is below 60 km/h. In this situation, an increase in the axial compressive force will emerge in the impacted pier owing

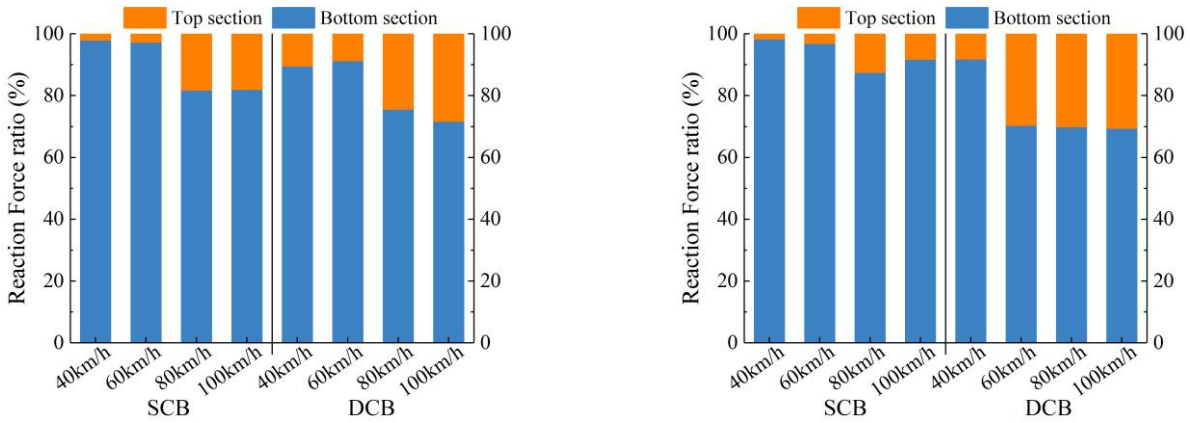

(a) 30 tons (b) 40 tons

Fig. 12 Ratio of the end reaction forces of the impacted piers under truck collision

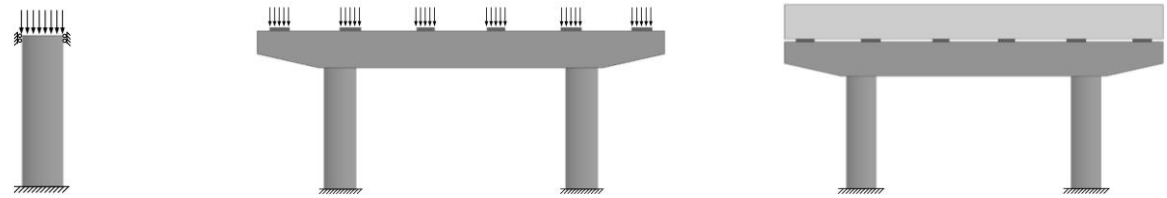

(a) Model 1 (b) Model 2 (c) Model 3

Fig. 13 Simplified bridge models

to the inertial force of the superstructure. In addition, when the truck hits piers at a higher velocity, an increase of the pier length is observed at the first impact stage; then, the pier head deforms downward due to its large lateral displacement in the subsequent impact stage. In this case, a large tensile force usually occurs in the pier, which may cause the tensile failure as shown in Fig. 8 (c)-(d). Moreover, it should be noted that, for the double-column bridge, the vertical displacement of the pier head decreases remarkably in the later impact stage owing to the constraint of the bent cap.

3.4 Internal force distribution

In the process of vehicle-bridge collision, shear failure is likely to occur at the base of the pier as a result of the large shear force transferred from the impact point in a very short time. Thus, the shear force at the pier end is also an important index to evaluate the impact capacity of the bridge structures. When the impact force reaches the maximum value, the ratios of the bottom and top section shear force to the total reaction force of the impacted piers under 30-ton and 40-ton truck collision are depicted in Fig. 12. The results show that the base of the pier resists most of the shear force induced by the impact action. The contribution of the top section increases with the HGV mass and velocity; however, the ratio of the top section is much less than that of the bottom section. For the single-column bridge, the maximum resistance provided by the inertial force of the superstructure and bent cap only reaches 20% of the total reaction force. In addition, even though with the supporting of the second pier, the top section shear force of the double-column bridge is also just 30% of the total reaction force. It is mainly because the impacted pier appears a large tensile stress during the collision process, which significantly reduces the section shear capacity. Anyway, compared with the single-column bridge, the double-column bridge can resist more impact action because of the reaction force provided by the bent and the second pier.

4. Behaviour of the simplified bridge models

As discussed above, the collision duration is so short that the local effect of the impact action on the structure is very significant. In general, only the impacted pier resists the impact force in the early impact stage. In order to reduce the modeling and computing cost, a discussion on the simplified methods for modeling bridge structures under HGV collision is carried out in this section. The double-column bridge is simplified into three pier-bent systems respectively: 1) Model 1 (refer to Fig. 13(a)), the bridge is simplified as a single pier. The translational degrees of freedom in horizontal direction of the pier head outer vertical faces are restrained, and an axial load is applied to the top of the pier which is equal to the equivalent gravity load of the superstructure. 2) Model 2 (refer to Fig. 13(b)), the vertical loadings are applied on the top of substructure to replace the gravity load of the superstructure. 3) Model 3 (refer to Fig. 13(c)), compared with the model 2, the superstructure is substituted with a rigid mass block.

To investigate the influence of the simplified methods on the dynamic behavior of the bridge structures, the FE model of the 40-ton truck-tractor-trailer is used to collide the bridge models at the impact velocities of 40 km/h, 60

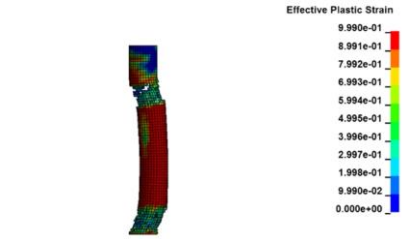

(a) Model 1

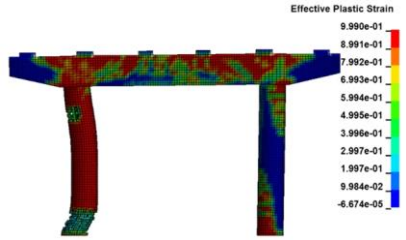

(b) Model 2

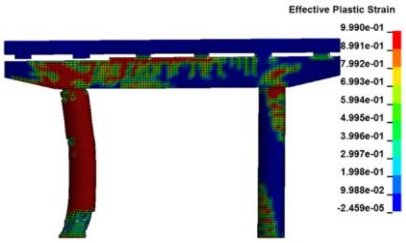

(c) Model 3

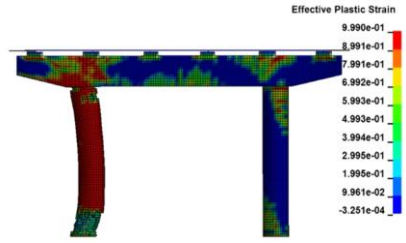

(d) Full bridge model

Fig. 14 Failure modes of the bridge models

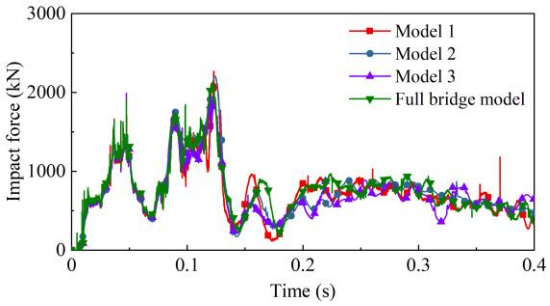

(a) 40 km/h

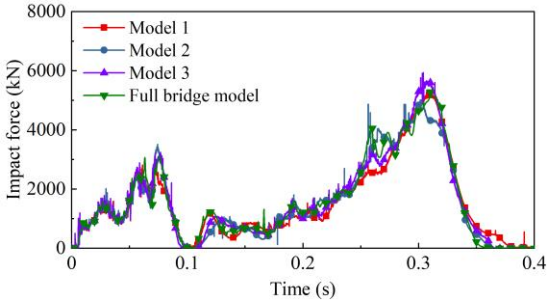

(b) 60 m/h

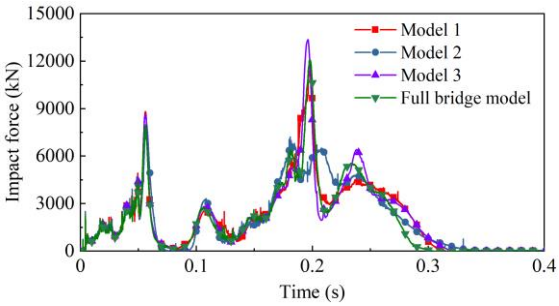

(c) 80 km/h

Fig. 15 Time histories of impact force at different velocities

km/h and 80 km/h, respectively. The failure modes, time histories of impact force, lateral deformation, internal force of the simplified models are compared with that of the full bridge model under different load cases.

4.1 Failure modes

Fig. 14 illustrates the failure modes of the bridge models under the HGV collision at the initial velocity of 80 km/h. It is observed that the bent cap and the second pier appear a certain degree of damage, besides both ends of the impacted piers are seriously damaged. This indicates that the second pier resists partial impact action in the collision process, due to the force-transferring mechanism of the bent cap. Moreover, the impacted piers experience the shear failure at the base. It also should be noticed that the tensile damage occurs near the top of the piers, especially for model 1. Among all the simplified models, model 1 exhibits more serious damage than the other bridge models, and the damage state of model 3 is more consistent with the full bridge model.

4.2 Impact force time histories

Fig. 15 plots the impact force time histories of the different models collided by the HGV at the impact velocities of 40 km/h, 60 km/h and 80 km/h. It can be observed that the impact force time histories have a great discrepancy at different velocities. A large spike is generated by the engine when the impact velocity is low, whereas the peak impact force is governed by the cargo impact action at high impact velocity. In the engine impact stage, the impact force time histories of the models are almost similar, due to the fact that the impacted pier has no time to response in a short time and the engine impact action is relatively small. However, when the cargo impacts the pier, the structural response will be affected by the structural properties and the damage degree. Therefore, there are some differences in the impact force time histories of the models in the cargo impact stage. With the increase of impact velocity, the difference in the impact force of the models becomes bigger in the cargo impact stage. In particular, the peak impact force of model 2 is greatly less than that of other models under the velocity of 80 km/h. The engine impact force under the velocity of 80 km/h is even large than the peak impact force under the velocity of 60

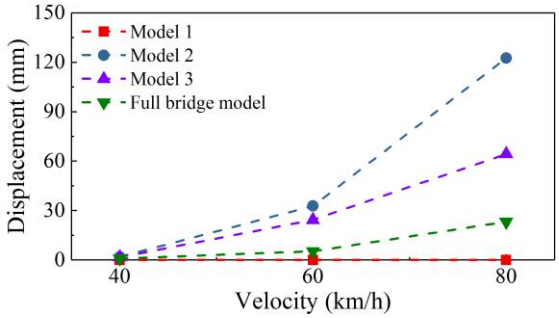

(a) Maximum displacement

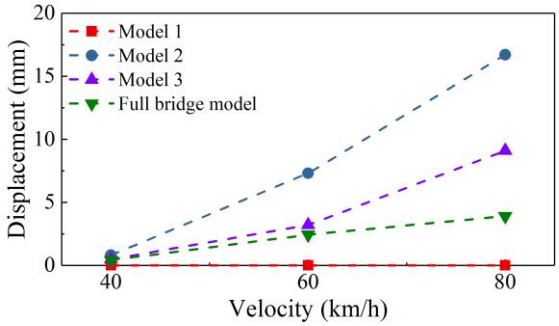

(b) Displacement at the peak impact force

Fig. 16 The pier top lateral displacements

km/h. Since model 2 lacks the resistance provided by the superstructure, most of the engine impact action is resisted by the pier. In this case, the pier of model 2 suffers more serious damage than other models and may not be able to resist the larger cargo impact action in the following impact stage. In this case, when the cargo impacts the pier, the pier lateral deflection of model 2 increases more quickly, which means the pier tends to separate from the vehicle. Thus, the peak impact force of model 2 is less than other models in the cargo impact stage. It is concluded that the simplified methods for modeling the superstructure have a slight effect on the impact force of bridges under the low-velocity collision. However, the constraint of the superstructure greatly affects the dynamic response of bridge structures under high-velocity impact. Therefore, under HGV collision at a low velocity, the full bridge model can be simplified as model 1 to obtain the impact force.

4.3 Top displacement

The top lateral displacement of the pier directly affects the bearing safety and the stability of the superstructure, so it is also an important index to evaluate the dynamic response of the bridge structures. Fig. 16 presents the maximum top lateral displacement and the top lateral displacement at the peak impact force in the different impact cases. As shown, the maximum top displacements of the impacted piers increase with the increasing impact velocity. Because of neglecting the inertial effect of the superstructure, the top lateral displacement of the model 2 is larger than that of other bridge models under the same impact action, especially at high impact velocities. It should be noticed that the lateral displacements are less than 18 mm at the peak impact force, which is much less than the maximum displacement of 130 mm.

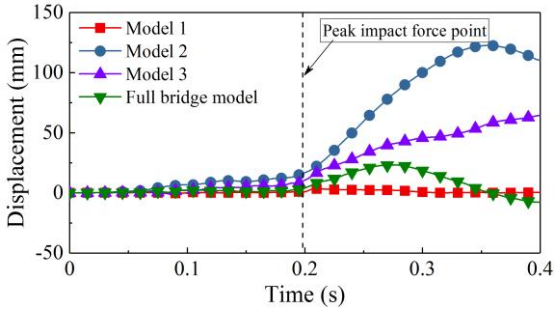

Fig. 17 The top lateral displacement time histories

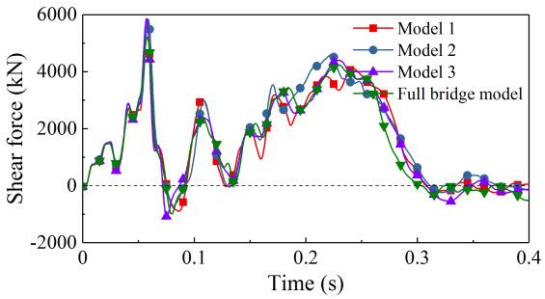

(a) Bottom section of the impacted pier

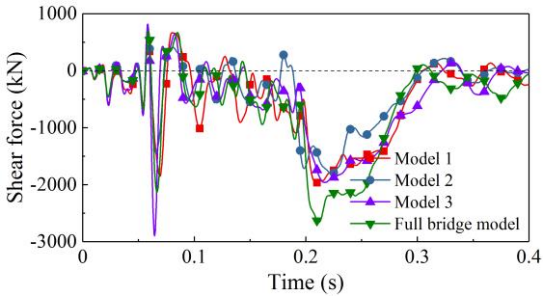

(b) Top section of the impacted pier

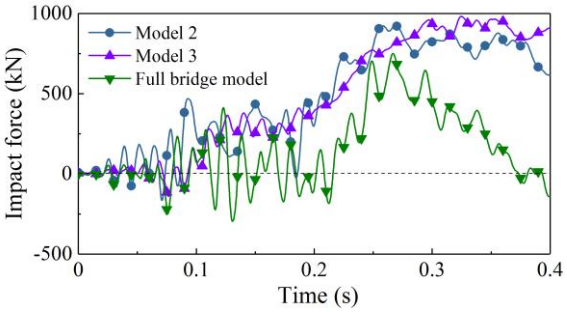

(c) Top section of the second pier

Fig. 18 Time histories of the section shear force

Fig. 17 shows the time histories of the top lateral displacement of the bridge models collided by the 40-ton HGV at the velocity of 80 km/h. It can be found that the top lateral displacements are very small before the impact force reaches the maximum value. After that, the other components of the bridges begin to participate in the impact respond, and finally the pier top displacement reach the maximum value. Moreover, the top lateral displacement of the full bridge model is negative after the impact time of 0.36 s, which indicts that the deck has a certain constraint effect on the overall response of the bridge structure.

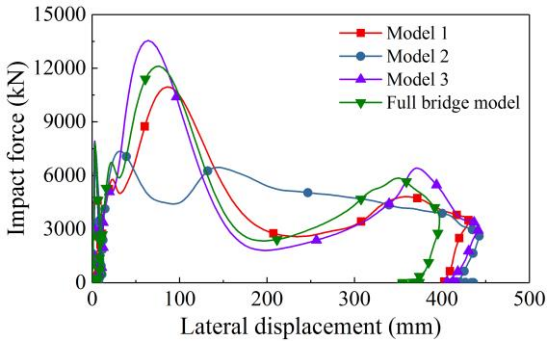

Fig. 19 Impact force versus lateral displacement

According to the discussion above, it can be concluded that the simplified methods have litter effect on the top displacement of the pier in the early impact stage but make a certain difference in the global response stage.

4.4 Section shear force

In order to evaluate the contribution of the second pier to the impact capacity of the bridge structure, the section shear forces at the pier end are investigated herein. The time histories of the section shear force of the impacted pier and second pier are shown in Fig. 18. For the impacted piers, the shear force at the base is about two times that of the top section, which indicates that most of the peak impact force is resisted by the pier base. Moreover, the end section shear forces of the different models are almost identical. However, the shear force of the second pier is smaller and lags far behind in the impact stage. Furthermore, it can be observed that the shear forces of the second pier of the model 2 and model 3 are different with that of the full bridge model, due largely to the various boundary condition of the superstructure. Fig. 19 presents the impact force versus central lateral displacement curves of the bridge models under the impact velocity of 80 km/h. The impact force versus lateral deflection curves of the model 1 and model 3 are close to the full bridge model. As the inertia effect of the superstructure is ignored, there is has a certain difference between model 2 and other bridge models.

As discussed above, the pier failure modes of the simplified models are nearly identical under the same impact action, even though there are some differences in the damage levels. The simplified method of the superstructure has an insignificant effect on the dynamic response of the bridge in the early impact stage but play an important role on the global response. It also can be concluded that the simplified methods have minor effect on the impact force under low-velocity impact cases. However, as the inertial effect of the superstructure is ignored, the peak impact force and lateral deformation of model 2 is different with other models. Therefore, to reduce the computing cost, the model 1 can be utilized to compute the impact force without a significant loss of precision. Thus, the dynamic response of the bridge structures subjected to the vehicle collision can be approximately investigated with model 3. If the computing cost is allowed, it is better to use the full bridge model to analyze the performance of the bridge structures.

5. Conclusions

In this paper, the impact behavior of the bridges with different structural types such as the single-column and double-column bridge subjected to HGV collision is numerically investigated. In addition, the effect of simplified methods for modeling bridge structures on the dynamic response of the bridges is also examined. The main conclusions are drawn as follows:

- Due to the high redundancy, the double-column bridge can delay the structural failure under the HGV collision, whereas the single-column bridge may directly collapse. Based on the performance-based design concept, the structural redundancy should be considered in the anti-impact design of the bridges.
- The impact mass, impact velocity and contact interface play dominated roles on the impact force. Under the high initial kinetic energy, the peak impact force is mainly determined by the stiffness and mass of the cargo; otherwise, the engine should be carefully considered in the impact analysis.
- The deformation behaviors of piers vary greatly with the bridge types. For single-column bridge, the pier deformation behavior is similar to that of a cantilever beam. However, the double-column bridge pier is more like a fixed-end beam. Under the HGV collision, the piers not only generate a large lateral displacement but also a significant axial displacement, which threaten the safety and stability of the bearing and superstructure. The bent cap of the multicolumn bridge can effectively restrict the displacement of the impacted pier.
- The simplified methods for modeling bridge structures have a slight effect on the impact force under the low-velocity impact but greatly affect the dynamic response of bridge structures under high-velocity impact. As the inertial effect of the superstructure is critical to the impact response of the bridges, it should be considered in the simplified model to explore the performance of bridges under vehicle collision.

Acknowledgments

The authors gratefully acknowledge the financial support provided by the National Science Foundation of China under Grant No. 51438010.

References

AASHTO-LRFD (2012), LRFD Bridge Design Specifications, American Association of State Highway and Transportation Officials, Washington DC, USA.

Abdelkarim, O.I. and ElGawady, M.A. (2016), "Performance of hollow-core FRP-concrete-steel bridge columns subjected to vehicle collision", *Eng. Struct.*, **123**, 517-531.

Abdelkarim, O.I. and ElGawady, M.A. (2017), "Performance of bridge piers under vehicle collision", *Eng. Struct.*, **140**, 337-352.

BS EN 1991-1-7:2006 (2006), Eurocode 1: Actions on Structures-Part 1-7: General Actions-Accidental Actions, British Standards Institution, London, UK.

Buth, C.E., Brackin, M.S., Williams, W.F. and Fry, G.T. (2011), "Collision loads on bridge piers: Phase 2", Report of Guidelines for Designing Bridge Piers and Abutments for Vehicle Collisions, Texas Transportation Institution, Texas, USA.

Buth, C.E., Williams, W.F., Brackin, M.S., Lord, D., Geedipally, S.R. and Abu-Odeh, A.Y. (2010), "Analysis of large truck collisions with bridge piers: Phase 1", Report of Guidelines for Designing Bridge Piers and Abutments for Vehicle Collisions, Texas Transportation Institution, Texas, USA.

Chen, L., El-Tawil, S. and Xiao, Y. (2016), "Reduced models for simulating collisions between trucks and bridge piers", *J. Bridge Eng.*, **21**(6), 04016020.

Chung, C.H., Lee, J. and Gil, J.H. (2013), "Structural performance evaluation of a precast prefabricated bridge column under vehicle impact loading", *Struct. Infrastr. Eng.*, **10**(6), 777-791.

Cook, W., Barr, P.J. and Halling, M.W. (2013), "Bridge failure rate", *J. Perform. Constr. Facil.*, **29**(3), 04014080.

El-Tawil, S., Severino, E. and Fonseca, P. (2005), "Vehicle collision with bridge piers", *J. Bridge Eng.*, **10**(3), 345-353.

Eurocode (1998), EN 1317-1 to 1317-5 Road Restraint System, European Committee for Standardization, Brussels, Belgium.

Flanagan, D. and Belytschko, T. (1981), "A uniform strain hexahedron and quadrilateral with orthogonal hourglass control", *Int. J. Numer. Meth. Eng.*, **17**(5), 679-706.

Ji, B.H. and Fu, Z.Q. (2010), "Analysis of chinese bridge collapse accident causes in recent years", *China Civil Eng. J.*, **43**(S1), 495-498. (in Chinese)

Jones, N. (2011), *Structural Impact*, 2th Edition, Cambridge University Press, New York, NY, USA.

JTG D60-2004 (2004), General Code for Design of Highway Bridges and Culverts, People's Communications Press, Beijing, China. (In Chinese)

JTG/T B02-01-2008 (2008), Guidelines for Seismic Design of Highway Bridge, People's Communications Press, Beijing, China. (in Chinese)

Kang, H. and Kim, J. (2017), "Response of a steel column-footing connection subjected to vehicle impact", *Struct. Eng. Mech.*, **63**(1), 125-136.

LS-DYNA (2006), Theory Manual Version 971, © Livermore Software Technology Corporation, California, USA.

Madurapperuma, M.A.K.M. and Wijeyewickrema, A.C. (2013), "Response of reinforced concrete columns impacted by tsunami dispersed 20' and 40' shipping containers", *Eng. Struct.*, **56**, 1631-1644.

Moutoussamy, L., Herve, G. and Barbier, F. (2011), "Qualification of *Constrained_Lagrange_In_Solid command for steel/ concrete interface modeling", *Proceedings of the 8th European LS-Dyna Conference*, Strasbourg, France, May.

Murray, Y.D., Abu-Odeh, A.Y. and Bligh, R.P. (2007*), Evaluation of LS-DYNA Concrete Material Model 159*, Federal Highway Administration, USA.

Qian, J., Wang, J., Zhao, W. and Zhou, D. (2016), "Time variation characteristics of impact force in collision of heavy vehicle to the bridge pier", *7th China-Japan-US Trilateral Symposium on Lifeline Earthquake Engineering*, Shanghai, China, June.

Sha, Y. and Hao, H. (2012), "Nonlinear finite element analysis of barge collision with a single bridge pier", *Eng. Struct.*, **41**, 63-76.

Sharma, H., Hurlebaus, S. and Gardoni, P. (2012), "Performance-based response evaluation of reinforced concrete columns subject to vehicle impact", *Int. J. Impact Eng.*, **43**, 52-62.

Thilakarathna, H.M.I., Thambiratnam, D.P., Dhanasekar, M. and Perera, N. (2010), "Numerical simulation of axially loaded concrete columns under transverse impact and vulnerability assessment", *Int. J. Impact Eng.*, **37**(11), 1100-1112.

Wang, W. and Morgenthal, G. (2017), "Dynamic analyses of square RC pier column subjected to barge impact using efficient models", *Eng. Struct.*, **151**, 20-32.

Wardhana, K. and Hadipriono, F.C. (2003), "Analysis of recent bridge failures in the United States", *J. Perform. Constr. Facil.*, **17**(3), 144-150.

Xu, L.J., Lu, X.Z., Guan, H. and Zhang, Y.S. (2013), "Finite-element and simplified models for collision simulation between overheight trucks and bridge superstructures", *J. Bridge Eng.*, **18**(11), 1140-1151.

Yi, N.H., Choi, J.H., Kim, S.J. and Kim, J.H.J. (2015), "Collision capacity evaluation of RC columns by impact simulation and probabilistic evaluation", *J. Adv. Concrete Technol.*, **13**(2), 67-81.

CC